

Review

Processes of the Reliability and Degradation Mechanism of High-Power Semiconductor Lasers

Yue Song^{1,2}, Zhiyong Lv³, Jiaming Bai⁴, Shen Niu^{1,2}, Zibo Wu⁵, Li Qin^{1,2}, Yongyi Chen^{1,2,6,*}, Lei Liang^{1,2}, Yuxin Lei^{1,2}, Peng Jia^{1,2}, Xiaonan Shan^{1,2,*} and Lijun Wang^{1,2,7,8}

¹ State Key Laboratory of Luminescence and Applications, Changchun Institute of Optics, Fine Mechanics and Physics, Chinese Academy of Sciences, Changchun 130033, China; songyue@ciomp.ac.cn (Y.S.); 13623558919@163.com (S.N.); qinl@ciomp.ac.cn (L.Q.); liangl@ciomp.ac.cn (L.L.); leiyuxin@ciomp.ac.cn (Y.L.); jiapeng@ciomp.ac.cn (P.J.); wanglj@ciomp.ac.cn (L.W.)

² Daheng College, University of Chinese Academy of Sciences, Beijing 100049, China

³ School of Physics and Microelectronics, Zhengzhou University, Zhengzhou 450001, China; lvzhiyong@stu.zzu.edu.cn

⁴ School of Physics, Jilin University, Changchun 130015, China; baijm1119@mails.jlu.edu.cn

⁵ School of Opto-Electronics Information Science and Engineering, Changchun College of Electronic Technology, Changchun 130061, China; wzb23923651592021@163.com

⁶ Jlight Semiconductor Technology Co., Ltd., Changchun 130102, China

⁷ Peng Cheng Laboratory, No.2, Xingke 1st Street, Nanshan, Shenzhen 518000, China

⁸ Academician Team Innovation center of Hainan Province, Key Laboratory of Laser Technology and Optoelectronic Functional Materials of Hainan Province, School of Physics and Electronic Engineering of Hainan Normal University, Haikou 570206, China

* Correspondence: chenyy@ciomp.ac.cn (Y.C.); shanxn@ciomp.ac.cn (X.S.); Tel.: +86-180-4304-7205 (Y.C.)



Citation: Song, Y.; Lv, Z.; Bai, J.; Niu, S.; Wu, Z.; Qin, L.; Chen, Y.; Liang, L.; Lei, Y.; Jia, P.; et al. Processes of the Reliability and Degradation Mechanism of High-Power Semiconductor Lasers. *Crystals* **2022**, *12*, 765. <https://doi.org/10.3390/cryst12060765>

Academic Editor: Hao-chung Kuo

Received: 30 April 2022

Accepted: 23 May 2022

Published: 26 May 2022

Publisher's Note: MDPI stays neutral with regard to jurisdictional claims in published maps and institutional affiliations.



Copyright: © 2022 by the authors. Licensee MDPI, Basel, Switzerland. This article is an open access article distributed under the terms and conditions of the Creative Commons Attribution (CC BY) license (<https://creativecommons.org/licenses/by/4.0/>).

Abstract: High-power semiconductor lasers have attracted widespread attention because of their small size, easy modulation, and high conversion efficiency. They play an important role in national economic construction and national defense construction, including free-space communication; industrial processing; and the medical, aerospace, and military fields, as well as other fields. The reliability of high-power semiconductor lasers is the key point of the application system. Higher reliability is sought in the military defense and aerospace fields in particular. Reliability testing and failure analysis help to improve the performance of high-power semiconductor lasers. This article provides a basis for understanding the reliability issues of semiconductor lasers across the whole supply chain. Firstly, it explains the failure modes and causes of failure in high-power semiconductor lasers; this article also summarizes the principles and application status of accelerated aging experiments and lifetime evaluation; it also introduces common techniques used for high-power semiconductor laser failure analysis, such as the electron beam-induced current (EBIC) technique and the optical beam-induced current (OBIC) technique, etc. Finally, methods used to improve the reliability of high-power semiconductor lasers are proposed in terms of the preparation process, reliability screening, and method application.

Keywords: high-power semiconductor laser; failure mechanisms; accelerated aging test; failure analysis techniques

1. Introduction

High-power semiconductor lasers have the advantages of small size, light weight, high electro-optical conversion efficiency, and easy monolithic integration, and are widely used in free-space communication; industrial processing; and the medical, aerospace, and military fields, as well as in other fields. High power characteristics and the long-term stability of the laser's wavelength and bandwidth are important prerequisites for the broad application of semiconductor lasers. Generally speaking, levels above 100 mW for narrow-stripe, single-mode devices and levels above 1 W for all other single- and multi-emitter

lasers can be considered to be high power [1]. The reliability of high-power semiconductor lasers is limited by the optical power density at the output facet, heat dissipation, and the current density in the semiconductor. Understanding the reliability and failure mechanisms of high-power semiconductor lasers is essential for the development of high-performance and highly reliable application systems.

Research on the degradation mechanisms of semiconductor lasers dates back to the 1960s. In 1966, internal self-damage in gallium arsenide lasers was investigated by D.P. Cooper et al. from Services Electronics Research Lab. Baldock, Herts, UK. They suggested that the damage occurred as a result of the interaction between a critical high flux density and some randomly distributed structural properties such as defects or diffusion irregularities [2]. In 1967, H. Kressel and H. Mierop from RCA Laboratories postulated that the catastrophic damage in a GaAs injection laser resulted from the effects generated by stimulated Brillouin emissions [3].

In the mid-1970s, the Nippon Telegraph and Telephone Corporation (NTT) and the Nippon Electric Corporation (NEC) in Japan formed two research groups for collaboration in the study of the reliability of semiconductor lasers for optical communications [4]. However, for the next two decades, reliability research studies were limited by the technology, and the degradation failure phenomenon was not fully understood at the atomic level [5,6]. In the 21st century, IBM Zurich Research Laboratory (Switzerland) [7–9], Sumitomo Electric Industries, Ltd. (Japan) [10], Agilent (USA) [11], and the American Aerospace Corporation [12] have conducted systematic studies on the reliability and degradation of semiconductor lasers. The degradation mechanisms are gradually being addressed.

Analysis of the failure mechanism of high-power semiconductor lasers is an important basis for studying their reliability. In this paper, the failure mechanisms of high-power semiconductor lasers are introduced in detail, including three failure modes and the causes of performance degradation, such as internal degradation, mirror facet degradation, electrode degradation, packaging-related degradation, and the influence of environmental factors. The principles of accelerated aging experiments in high-power semiconductor lasers and their applications are also summarized. Failure analysis techniques such as the electron beam-induced current (EBIC) technique, the optical beam-induced current (OBIC) technique, the thermally induced voltage alteration (TIVA) technique, electroluminescence (EL), microphotoluminescence mapping (μ -PL), emission microscopy (EMMI), cathodoluminescence (CL), electron channeling contrast imaging (ECCI), transmission electron microscopy (TEM), and Raman are introduced in detail. The advantages and limitations of each technique are compared. Finally, methods by which to improve the reliability of high-power semiconductor lasers are proposed in terms of the preparation process, reliability screening, and method application. It is hoped that this study can provide a reference for research on the failure mechanisms of high-power semiconductor lasers, as well as improvements to their reliability.

2. Failure Mechanism

The performance of semiconductor lasers decreases with an increasing operating time. The most obvious manifestation of this is the decrease in output power and electro-optical conversion efficiency of the semiconductor laser at a constant drive current. In addition, catastrophic damage to the laser leads to a sudden drop in optical power [13]. Therefore, an increase in the drive current is required to prevent the degradation of the laser during constant power operation. The change in output power during laser degradation is mainly caused by the decrease in the lifetime of the injected carriers and the increase in internal optical losses. The mathematical model of the optical power output of a semiconductor laser is as follows [1]:

$$P_{out} = \eta_e (I - I_{th}) \frac{\hbar\omega}{q} \quad (1)$$

$$\eta_e = \eta_i \frac{\alpha_m}{\alpha_m + \alpha_i} \quad (2)$$

$$\alpha_m = \frac{1}{2L} \ln \frac{1}{R_1 R_2} \quad (3)$$

where P_{out} is the optical output power, η_e is the external differential quantum efficiency, I is the drive current, I_{th} is the threshold current, q is the electron charge, and $\hbar\omega$ is the energy quantum. η_i is the internal differential quantum efficiency; α_i is the internal loss, mainly caused by the free-carrier absorption of the waveguide material and the scattering loss due to the roughness of the optical waveguide layer; and α_m is the mirror loss. L is the cavity length, R_1 and R_2 are the front cavity mirror reflectivity and the rear cavity mirror reflectivity, respectively. Then, the root cause parameters directly affecting the decrease in output power are the increase in the threshold current and the decrease in the slope efficiency or external differential quantum efficiency.

2.1. Failure Mode

In most operating systems, semiconductor lasers usually operate at a constant output power and lasing wavelength. Therefore, when degradation occurs, variations in the drive current show different patterns, as shown in Figure 1.

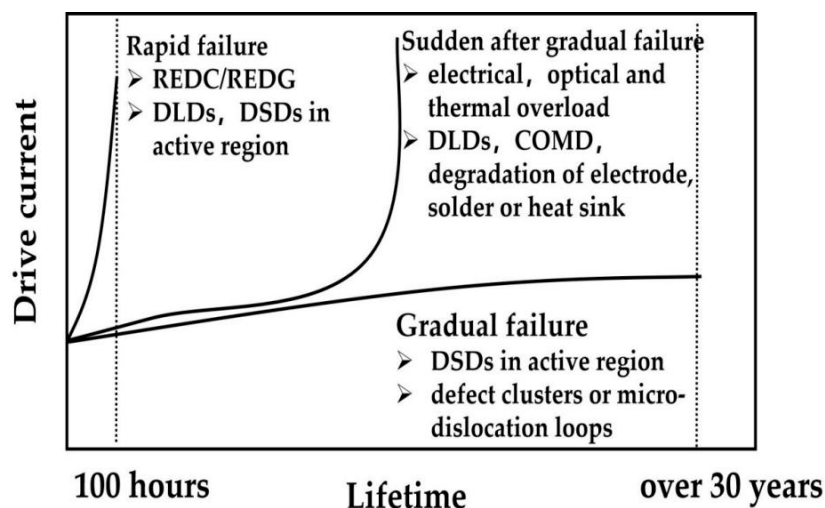


Figure 1. Failure mode of the laser diode at constant output power.

The failure modes of high-power semiconductor lasers are similar to those of ordinary semiconductor lasers. According to the relationship between drive current and lifetime, the failure modes of high-power semiconductor lasers are manifested in the following three forms: rapid failure, gradual failure, and sudden failure after gradual failure [14].

2.1.1. Rapid Failure

Rapid failure is usually observed within the first hundred hours of operation of a semiconductor laser. It manifests itself as a rapid drop in the output power and a rapid increase in the threshold current. Rapid failure is associated with defects present within the laser. These defects are introduced during the epitaxial growth of the wafer or the fabrication of the chip. The defects (such as the precipitation of impurity atoms and dislocations) are accelerated by non-radiative recombination processes; there is also vibration energy generated by recombination-enhanced dislocation climb or glide (REDC or REDG) [15,16]. As defects propagate in the diode structure, dislocation networks form and grow in the crystal structure, and these defects can destroy the active region of the semiconductor laser and make the laser ineffective. The types and formation mechanism of defects in degraded high-power semiconductor lasers are shown in Table 1 below.

Table 1. Defect types in degraded high-power semiconductor lasers.

Lasing Wavelength	Semiconductor Lasers	Defect Types	Mechanism
440–450 nm	InGaN/GaN QW lasers	<11-20> a-type dislocations [17]	Climb mechanism involving point defect
808 nm	AlGaAs/GaAs QW-SCH lasers	<110> DLDs Dislocations dipoles [18]	Gliding mechanism
980 nm	InGaAs/AlGaAs QW lasers	<100> DLDs Dislocation dipoles or climbed dipoles [18] <1-10> DLDs Edge dislocation dipoles	Climb mechanism involving point defect Gliding mechanism not involving point defect
1300 nm	InGaAsP/InP QW lasers	<100> DLDs Dislocation dipoles [19]	Climb mechanism involving point defect
1550 nm	InGaAs/InP QW lasers	V-shaped defects DLDs Misfit dislocations [20]	Climb mechanism

To eliminate rapid failure, it is necessary to apply low-defect or defect-free substrates to eliminate dark-line defects (DLDs) or dark-spot defects (DSDs) formed by the REDC or REDG mechanism. In addition, the selection of lattice-matched epitaxial films to reduce internal stresses in the laser structure and the selection of a support solder to reduce external stress during bonding are useful methods. Last but not least, avoiding defect formation during the epitaxial growth and fabrication processes is very important for reducing the probability of rapid failure.

2.1.2. Gradual Failure

This failure mode manifests itself in several forms, including a gradual and slow long-term decrease in the optical output power, and an increase in the threshold current with an increasing operation or aging time. To reach a certain output power, the drive current of the semiconductor laser needs to be increased. During this degradation process, the slope efficiency of the laser remains constant, and, for a constant drive current, the output power of the laser experiencing this failure mode can be seen to decrease over time. In general, the optical power of the laser must be recovered at the cost of a higher drive current [21]. The gradual failure mode often determines the maximum operating lifetime of semiconductor lasers. The mechanism of gradual failure is related to the enhancement of internal stress and the increase in non-radiative recombination centers in the active region. This failure is always associated with the formation of DSDs, caused by the growth of dislocation networks, and internal stresses, which are caused by defect clusters or micro-dislocation loops in the active region of high-power semiconductor lasers [4].

To avoid the gradual failure of semiconductor lasers, it is important to reduce the formation of non-radiative deep-level defect centers during epitaxial growth and device fabrication [22]. For example, a diffusion barrier layer is created during the preparation of metal electrodes to eliminate the inter-diffusion of metals and semiconductor materials.

Elimination of internal and external stresses around the active region, such as the selection of an appropriate strained quantum well (QW) structure, is an effective way to avoid long-term degradation. When the thickness of the QW layer is designed below a certain level, no misfit dislocation is formed due to strain relaxation. A heat sink material with a coefficient of thermal expansion that matches that of the semiconductor laser chip should be selected.

2.1.3. Sudden Failure after Gradual Failure

Sudden failure after gradual failure is manifested by a semiconductor laser that has been operating for a long period under normal operating conditions, but suddenly has no

light intensity output. This is the most serious failure mode in high-power semiconductor lasers. Sudden failure after gradual failure in most devices is associated with DLDs [23]. This degradation mode is closely related to electrical, optical, and thermal overloads and also limits the maximum power of high-power semiconductor lasers. In addition, catastrophic optical mirror damage (COMD) and electrode, solder, or heat sink degradation may also lead to sudden failure after gradual failure [24].

Effective cavity surface passivation methods, vacuum cleavage, and coating techniques or the fabrication of non-absorbing mirror structures, such as the use of QW intermixing technologies, are applied to prevent the COMD phenomenon. Appropriate composite heat sinks with high thermal conductivity and less thermal expansion stress can effectively improve the reliability of semiconductor lasers due to their good matching of thermal expansion efficiency to the chip.

2.2. Reasons for Degradation

As with many other types of electronic devices, the reliability and lifetime of high-power semiconductor lasers depend heavily on their operating conditions, the suitability of the epitaxial materials, and device structure. The high optical power density at the output facet, heat accumulation, and the large current density in the semiconductor have a significant influence on the reliability of high-power semiconductor lasers. Depending on the type and location of the degradation in semiconductor lasers, degradation can be classified as internal, mirror facet, electrode, degradation related to packaging, and degradation caused by environmental factors.

2.2.1. Internal Degradation

As the operating time increases, local gain saturation or the spatial hole burning effect lead to the formation of filamentation, self-focusing, or thermal lensing in the chip. Optically induced heating enhances defects, which are introduced by the substrate, epitaxial growth, or fabrication processes migrating to the active region. The non-radiative recombination rate of the carrier is accelerated [12]. The energy generated by the non-radiative recombination process is converted into an Auger recombination or lattice vibrations, leading to recombination-enhanced defect reactions (REDRs). The propagation of defects through the REDC and REDG mechanisms leads to the formation of dislocation networks known as DLDs [4]. The REDR process is further enhanced by the strong optically induced heating phenomenon. The slow propagation of internal defects within the epitaxial material leads to an increase in non-radiative recombination centers in the active region, accompanied by a decrease in the electro-optical conversion efficiency and the output power. As a result, degradation of the semiconductor laser occurs. Internal degradation also includes DLDs and DSDs, which often lead to the rapid failure of semiconductor lasers. Figure 2 shows a TEM image of a typical DLD observed in a rapidly degraded GaAlAs/GaAs double-heterojunction laser [25]. DLD can also cause catastrophic optical bulk damage (COBD), leading to the rapid failure of the laser [26]. COBD refers to the catastrophic damage occurring inside the laser, which is different from that on the mirror facet.

2.2.2. Mirror Facet Degradation

Mirror facet degradation is a serious problem for high-power semiconductor lasers. It is a combination of COMD and chemical corrosion. COMD is considered one of the major limiting factors for achieving ultra-high optical power and is the main bottleneck limiting its reliability [27].

Figure 3 below illustrates the process of COMD generation, which is directly caused by high cavity surface temperatures. The relevant heating mechanism is the non-radiative recombination process induced by impurity oxides formed at the cleaved facet surface and the strong optical absorption process of the emitted laser light [28].

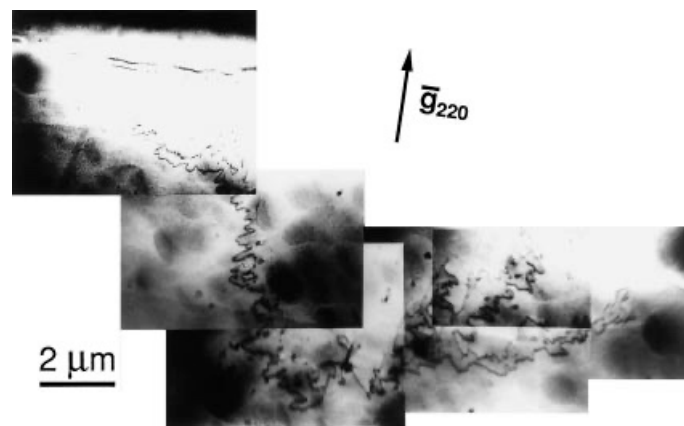


Figure 2. TEM image of dislocation dipole associated with $\langle 100 \rangle$ direction DLD in a rapidly degraded GaAlAs/GaAs double-heterojunction laser. Reprinted with permission from ref. [25] © Elsevier. Copyright 1999 Microelectronics Reliability.

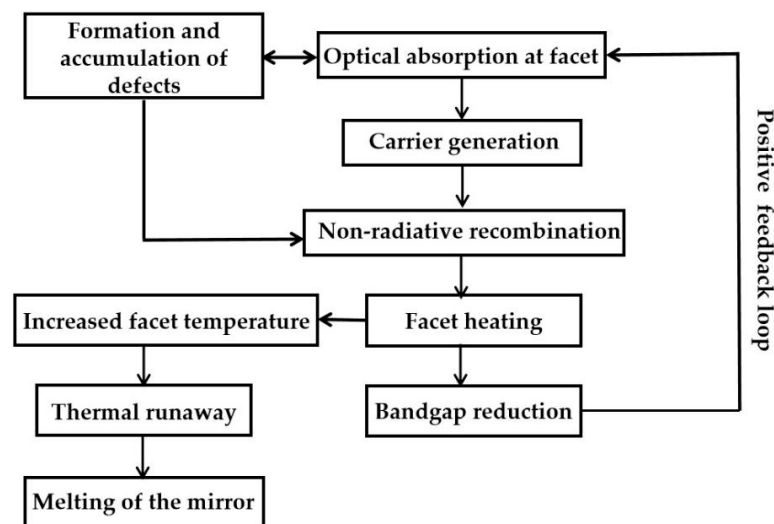


Figure 3. COMD generation mechanism.

In addition, the type of package may lead to an increase in the cavity surface temperature: packages of semiconductor lasers usually have an “overhang” of about $10\ \mu\text{m}$ to protect the mirror facet’s desorption from the solder material. As a result, the temperature of the mirror facet may be higher than that of the cavity [29]. The critical local temperature may be reached when the temperature is further increased by increasing the operating current or heat sink temperature, or when defects caused by aging are generated by long-term operation. At this point, intrinsic or extrinsic mechanisms leading to additional temperature increases from a positive feedback loop and thermal runaway start to occur.

When COMD occurs, DLDs are generated during the laser’s operation; these DLDs are areas of non-radiative combination centers in the active region of the laser; they are generated locally, both on the cavity surface and inside the cavity, and can propagate along the cavity driven by the optical field, eventually leading to laser failure.

The photochemical action leads to slow oxidation of the mirror facet, which, in turn, leads to a gradual increase in local defects on the cavity surface and a change in their corresponding local reflection coefficients. An increase in optical absorption at the defects leads to an increase in local non-radiative recombination and a corresponding increase in temperature. Semiconductor lasers containing aluminum in the active region are more susceptible to catastrophic damage because aluminum adsorbs water and oxygen, making the laser cavity surface more susceptible to oxidation, which leads to the formation of local defects, and the device suffers catastrophic damage with increasing operation time.

2.2.3. Electrode Degradation

The main causes of electrode degradation are the degradation of ohmic contact and the degradation of thermal resistance. Ohmic contact degradation is mainly due to ion diffusion and electrical migration between the electrode material and the semiconductor material. In order to obtain a high output power, the electrodes of semiconductor lasers usually operate at very high current densities. At high current densities, electrical migration of metal ions in the electrodes occurs [30]. Metal ions undergo directional migration driven by high-density electron flow, and undergo significant mass transport, which, in turn, creates cavities voids or mounds (or whiskers) in the contact structures of the metal and semiconductor materials, producing electromigration failures. Electromigration failure often occurs together with processes such as chemical migration, stress migration, and thermal migration [31], leading to degradation failure of the electrode. In addition, impurity particles introduced during the welding process, as well as thermal stresses due to excessive temperature rising and falling, can also lead to degradation of the electrode.

2.2.4. Packaging-Related Degradation

The packaging stresses generated during the manufacturing process of a high-power semiconductor lasers can seriously affect their service life. Encapsulation stress is mainly caused by the mismatch of thermal expansion coefficients between the chip and the heat sink materials. Encapsulation stress changes the bandwidth of the semiconductor material and introduces a large number of dislocations in the active region, affecting the threshold current, wavelength, linewidth, and polarization of the laser [32]. Then, the service life of the laser is reduced, leading to transient failure. Solder (e.g., indium) creeps and climbs during operation, accumulating at the mirror facet and causing side leakage, leading to short circuits. Gaps created during the soldering process and oxidation of the solder can lead to laser degradation.

2.2.5. Influence of Environmental Factors

High-power semiconductor lasers are widely used in both terrestrial and space systems. For application scenarios in space systems, the exacerbating effect of radiation damage from the environment on laser degradation needs to be considered. Proton irradiation [33], electron irradiation [34], and γ -ray irradiation [35] can lead to crystal defects in semiconductor materials (e.g., Frenkel-type defects), which can affect the reliability of semiconductor lasers. The ambient temperature range for terrestrial systems is typically -40 to $+85$ °C. The temperature conditions in space are much harsher than those in terrestrial applications, e.g., from -120 °C to $+120$ °C. A drastic temperature variation range can also deteriorate the reliability.

The reliability of high-power semiconductor lasers can also be greatly affected by electrostatic discharge damage (ESD) generated during manufacturing, transportation, and use. ESD damage is typically caused by one of three events: direct static electricity from a person to a device, static electricity from a charged device, or field-induced discharge. Therefore, suitable models for simulating ESD-induced damage are called the Human Body Model (HBM), the Charged Device Model (CDM), and the Machine Model (MM), respectively. High-power semiconductor lasers are classified into edge-emitting lasers (EELs) and vertical cavity surface-emitting lasers (VCSELs) according to the emitting direction. VCSEL and VCSEL arrays are extremely sensitive to ESD [36,37]. If an ESD event occurs, catastrophic damage in the active area may occur leading to sudden failure of the semiconductor laser, and the laser may then degrade in its subsequent operation with the occurrence of other failure mechanisms, which can be easily confused with other causes of failure.

3. Accelerated Aging Test and Lifetime Test Method

3.1. Reliability

3.1.1. Reliability Overview

Reliability is the ability of a product to perform a “specified function” under “specified conditions” and for a “specified time”. Reliability is usually reflected indirectly by the failure rate. According to Equation (1), failure of a semiconductor laser is generally defined as a failure when the drive current I remain constant and the output power P_{out} decreases to a certain percentage (e.g., 50% of the initial value, which can also be specified), or when the output power P_{out} remains constant and the drive current I rises to a certain degree (e.g., 120% of the initial value).

The failure rate of a semiconductor laser (instantaneous failure rate) $\lambda(t)$ is the probability of failure per unit of time after the laser has been in operation up to the moment t .

Figure 4 shows a typical failure rate function for a 1550 nm distributed feedback (DFB) laser [38].

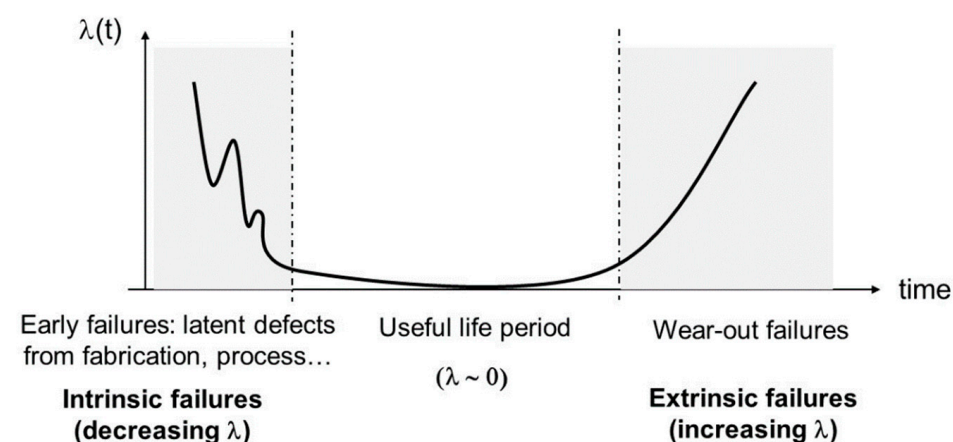


Figure 4. Variations of the time-dependent failure rate. Reprinted with permission from ref. [38] © Elsevier. Copyright 2021 Advanced Laser Diode Reliability.

The failure pattern of most optoelectronic devices is similar to this curve and is divided into three phases called the early failure period, the random failure period, and the wear period.

- (1) Early failure: The device has a high failure rate and a very short operating lifetime, usually due to rapid degradation caused by the rapid growth of the internal defects within the device. These defects are mainly generated during the manufacturing process.
- (2) Random failure: This stage has a low failure rate, is difficult or impossible to predict, and is associated with chance factors.
- (3) Wear and tear failure: The device shows wear and ages in different operating environments, reaching its service life, and eventually failing.

3.1.2. Reliability Experiments

Reliability experiments are an important method by which to study the reliability of high-power semiconductor lasers. Reliability experiments are divided into four main categories: environmental experiments, lifetime experiments, special test experiments, and field application experiments. The lifetime of a high-power semiconductor laser is an important indicator of its reliability. Lifetime experiments are common methods used to evaluate the reliability and degradation analysis of semiconductor lasers.

The lifetime experiments are divided into long-term lifetime experiments and accelerated aging experiments. With the development of high-power semiconductor lasers, their lifetimes have been continuously improved, and most of them have reached a lifetime on the order of 10,000 h. If the lifetime experiment is completed according to an actual application environment, the test time can be long and the device cost can be high. In order

to save time and costs, accelerated aging experiments are often used to quickly determine the reliability of the device.

3.2. Accelerated Aging Experiment

3.2.1. Theoretical Basis for the Accelerated Aging Test

The idea of the accelerated aging experiment is to create an experimental environment at high stress levels, so the necessary experimental data of the test device can be obtained. Then, one can apply statistics or other data processing methods to extrapolate the lifetime characteristics of the device operating at normal stress [39]. Therefore, the relationship between lifetime characteristics and stress levels needs to be established. The common accelerated stresses used in aging experiments of high-power semiconductor lasers are mainly temperature stresses and electrical stresses.

Arrhenius Model

An important model is the Arrhenius equation that expresses the temperature stress and reaction rate as follows [40]:

$$\frac{dM(T)}{dt} = A_0 \exp\left(\frac{-E_a}{kT}\right) \quad (4)$$

$\frac{dM(T)}{dt}$ is the rate of process to failure, indicating the speed of the reaction; k is the Boltzmann constant; E_a is the activation energy that causes the failure or degradation process; T is the absolute temperature; and A_0 is a non-thermal constant factor. A cumulative failure distribution diagram at different constant temperatures is usually used to obtain the median life (mean time to failure) at each temperature. According to the Arrhenius curve of median life and temperature, the failure activation energy and the extrapolated working life of the devices can be obtained.

Inverse Power Law Model

When the life of a system is an inverse power function of the accelerating stress variable, the inverse power law is commonly used. The inverse power law model describes the relationship between the applied stresses (e.g., voltage, current, optical power, temperature cycling, or mechanical vibration, etc.) and the lifetime of a semiconductor laser [41].

$$L_s = Av^{-C} \quad (5)$$

L_s represents the life at a stress of v ; A is a constant typical for laser type; C is an exponent characteristic of the laser device, which is a positive constant related to the activation energy; and v is the accelerating stress.

Different stresses produce different failure mechanisms, and the choice of stresses in the experiment is determined by the actual situation. The Arrhenius model and the inverse power law model can be linearized and written uniformly in the following form:

$$L_s = a + b \ln \phi(s) \quad (6)$$

L_s is the characteristic lifetime; ϕ is a function related to the s stress; and a and b are coefficients that can be calculated from the experimental data.

3.2.2. Classification of Accelerated Aging Test

The accelerated aging test can be divided into constant stress, step stress, and sequential stress accelerated aging experiments according to the variation law of the accelerated stress applied in accelerated aging experiments [42].

Constant stress experiments are performed by dividing the stress levels into different groups and then testing the devices in different groups until all the devices fail. The stress level does not change during the whole experiment.

Step stress experiments are also divided into different stress levels. All the test devices are placed at the same level. After a period of time, the stress level is switched to a higher level. The failed devices are removed, then the experimental conditions are switched to another higher stress level, and so on, until a certain percentage of devices fail.

The sequential stress experiment is similar to the step stress experiment, except that the stress level of the sequential stress experiment increases continuously with time, which can also be regarded as the limiting case of the step stress, in which the time interval of the stress transition is considered to be very small.

Among these three experimental methods, the experimental environment setting of the constant stress experiment is relatively simple, but the test is very time-consuming; the experimental operation of the step stress experiment is more complicated than that of a constant stress experiment, but it is more time saving. The experimental environment setting of the sequential stress experiment is complicated, and there are fewer related reports.

3.3. Example of Accelerated Aging Test

Research on the lifetime of high-power semiconductor lasers around the world has focused on several large laser manufacturing companies and research institutions, such as IBM Zurich Research Laboratory [43,44], NASA [45,46], COHERENT [47], JOLD in Germany [48], the 13th Research Institute of China Electronics Technology Group Corporation [49], the Research Institutes of Chinese Academy of Sciences [50], nLight Corporation [51,52], and the American Aerospace Corporation [53,54], etc.

In 1991, A. Moser and E.E. Latta of the IBM Research Division, Zurich Research Laboratory, determined the apparent Arrhenius parameters for the rate process of COMD failure. They compared the rate processes for various cleaved facets with and without a subsequent plasma oxidation step. A tentative model for facet heating that ultimately leads to COMD in AlGaAs/GaAs QW lasers was established [43].

In 1994, A. Oosenbrug and E.E. Latta of the IBM Research Division, Zurich Research Laboratory studied the high-power operational stability of 980 nm InGaAs/AlGaAs QW lasers. In total, 60 high-power semiconductor lasers were tested for their long-term lifetimes, with individual hours ranging from 6000 to 32,000 h, some at power levels above 200 mW (up to 300 mW continuous wave). For a group of devices operating at 200 mW continuous wave and at 50 °C, they found a log-normal distribution with a median life of >150 kh [44].

In 2005, Guoguang Lu et al. of Changchun Institute of Optics and Mechanics, Chinese Academy of Sciences, investigated the reliability of 808 nm high-power InGaAsP/InP lasers using constant stress accelerated aging tests [49]. They conducted constant current aging tests on six randomly selected lasers at 70 °C and 80 °C with an operating current of 1000 mA, and used the Arrhenius equation to derive a lifetime of 30,000 h at 25 °C.

In 2008, Hongde Wang et al. of the 13th Research Institute of China Electronics Technology Group Corporation conducted aging experiments on 808 nm AlGaInAs/AlGaAs/GaAs QW lasers [50]. They performed step stress experiments based on the inverse power law model, with electrical stress levels of 1, 1.3, 1.5, 1.7, and 2 A for a duration of 600 h. By comparing the failure rates of the devices with constant stress and step stress experiments, they found the same failure modes and similar lifetime estimates for both methods. This experiment verified that the step stress test is more time efficient than the constant stress test.

In 2011, nLight corporation performed reliability tests on 976 nm single-emitter laser diodes [51,52]. Seven sets of test conditions were performed: 18 A, 52 °C (drive current, junction temperature); 12 A, 62 °C; 16 A, 55 °C; 14 A, 58 °C; 15.7 A, 88 °C; 15 A, 73 °C; and 13.7 A, 42 °C. Over 15,000 h of accelerated life test reliability data were collected. The effects of temperature and power acceleration were evaluated by accelerated aging tests, and it was concluded that the mean time to failure was greater than 30 years at an output power of 10 W and a junction temperature of 353 K (80 °C), with a statistical confidence level of 90%.

In 2016, the American Aerospace Corporation reported their study of long-term accelerated aging tests on high-power, single-mode and multi-mode InGaAs/AlGaAs strained QW lasers [53,54]. They tested 64 single-mode 975 nm QW lasers with four experimental conditions: a drive current of 1.5 A and a junction temperature of 70 °C; a drive current of 1.5 A and a junction temperature of 120 °C; a drive current of 1.8 A and a junction temperature of 70 °C; a drive current of 2.1 A and a junction temperature of 70 °C. The test time for each test condition was 6500 h, and the test accumulation was 25,000 h (nearly 3 years). They tested 32 multi-mode lasers with lasing wavelengths of 920–960 nm at a drive current of 4 A and a junction temperature of 55 °C, for a total of over 35,000 h. This is the longest reported lifetime test for a single-mode or multi-mode laser in the 915–980 nm band. Their failure analysis of the devices showed that the main cause of failure was internal degradation.

In 2017, Zhiwen Wang et al. of the Institute of Semiconductors, Chinese Academy of Sciences, conducted a lifetime test of their self-developed 975 nm high-power semiconductor laser using a current step stress aging experiment [55]. They set the current stresses to 10, 12, and 14 A, and the aging times to 1200 h, 500 h, and 500 h. The test results were analyzed according to the inverse power law model, and the average lifetime of the device at a current of 8 A was calculated to be 28,999 h.

In 2019, constant temperature and constant current aging tests were conducted on 18 conduction-cooled packaged 60 W 808 nm high-power diode lasers by the Xi'an Institute of Optics and Precision Mechanics, Chinese Academy of Sciences, and Xi'an Focuslight Technologies Inc [56]. The average laser lifetime was 1022, 620, and 298 h at three different heat sink temperatures of 55, 65, and 80 °C with a constant current of 60 A. The lifetime at room temperature was calculated to be 5762 h according to the Arrhenius formula. The number of lasers in this experiment was relatively large, and the test temperature and output power were high. Because of the high costs and long duration of this experiment, such reports are quite rare.

4. Failure Analysis Techniques

The performance and reliability of semiconductor lasers can be significantly improved by precisely defining the location and cause of damage. Many techniques have been employed to characterize the failure modes and degradation mechanisms of high-power semiconductor lasers: the EBIC technique, the OBIC technique, the TIVA technique, EL, μ -PL, EMMI, CL, ECCI, TEM, and Raman, etc.

4.1. EBIC

EBIC is a technique commonly used to detect defect localization in semiconductor lasers for in-depth failure analysis [57,58]. It is a scanning electron microscopy (SEM)-based technique used to measure the current flowing through a semiconductor. When an electron beam is shone on a semiconductor chip, electron–hole pairs are created in a certain range within the semiconductor. The induced current of carriers can be collected by the internal electric field, which detects electrical defects with reduced carriers due to recombination. The intensity of the EBIC signal corresponds to the strength of the internal electric field around the p–n junction. Defects that are non-radiative recombination centers show a significantly lower EBIC signal [59,60].

Since the depth of the generated carriers depends on the accelerating voltage, a wide voltage range from 5 to 40 kV is essential for the quantitative study of the defect activity. Typically, the lateral resolution of EBIC varies from 20 to 500 nm, depending on the SEM conditions and material composition.

In 2018, Yong Kun Sin et al. from the California Aerospace Corporation EI Segundo, employed the EBIC technique for the first time to determine the failure modes of 980 nm degraded single-mode InGaAs/AlGaAs strained QW lasers by observing DLDs [61]. Figure 5 shows the EBIC images of the high-power InGaAs/AlGaAs QW laser under different aging conditions: (a) 2.1 A/70 °C with a fail time of 10,205 h, (c) 1.8 A/70 °C with a fail

time of 2560 h, and (d) 2.1 A/70 °C with a fail time of 1180 h. This clearly shows that the onset of the DLDs is confined within the 4 μm wide waveguide. The combination of the SEM and EBIC images indicates that the degradation process occurs in the active layer.

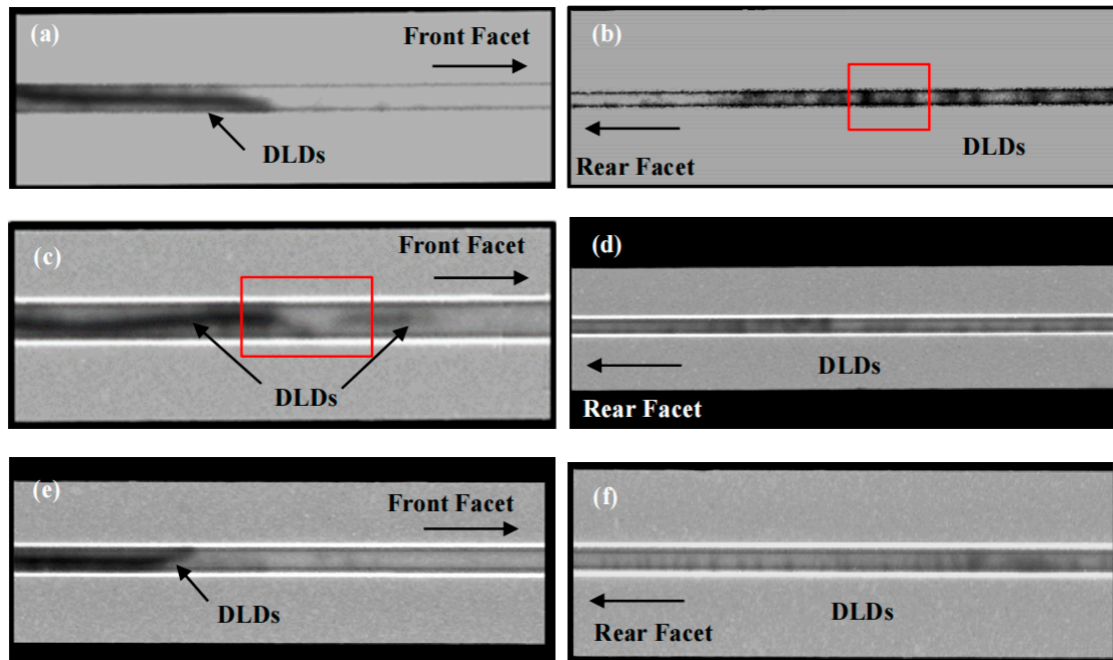


Figure 5. EBIC images were captured from high-power InGaAs/AlGaAs QW lasers with different aging conditions near the front facet. (a) 2.1 A/70 °C with a fail time of 10,205 h, (c) 1.8 A/70 °C with a fail time of 2560 h, and (e) 2.1 A/70 °C with a fail time of 1180 h and corresponding EBIC images near the rear facet (b,d,f). Reprinted with permission from ref. [61] © SPIE. Copyright 2018 Proceedings of SPIE.

In 2020, the rapid degradation behavior and failure mechanisms of InGaN/GaN green laser diodes (LDs) were investigated by the University of Shanghai for Science and Technology and the Chinese Academy of Sciences using the EBIC technique to assist in identifying the location of defects [62]. The SEM and EBIC images of the non-aged LD are shown in Figure 6a,d, and the SEM images of the two possible locations where the LD underwent severe degradation after the aging experiments are shown in Figure 6b,c. Compared with the non-aged LD, bubble-like defects can be observed in the images marked as P1 and P2, in which, combined with Figure 6e,f, the EBIC signal is slightly reduced. According to the EBIC principle, a higher carrier trap density exists in the active region of the laser near the bubble-like defects.

4.2. OBIC

OBIC is a non-destructive, highly sensitive, and high-resolution technique that is widely used to characterize defects present in semiconductor lasers such as stacking faults, dislocations, diffusion spikes, diffusion pipes, electrical over stress (EOS), and ESD damage. OBIC is a scanning optical microscopy imaging mode that locates regions of Fermi-level transitions. When the active region of a semiconductor laser is illuminated by a focused and scanned beam, the electron–hole pairs generated in the active region are separated by the built-in electric field in the p–n junction, and then collected by the electrodes to form a photocurrent that serves as the OBIC signal. Defects in the semiconductor material produce local variations in the Fermi level or the built-in potential that can enhance or weaken the recombination current, and, hence, the OBIC signal.

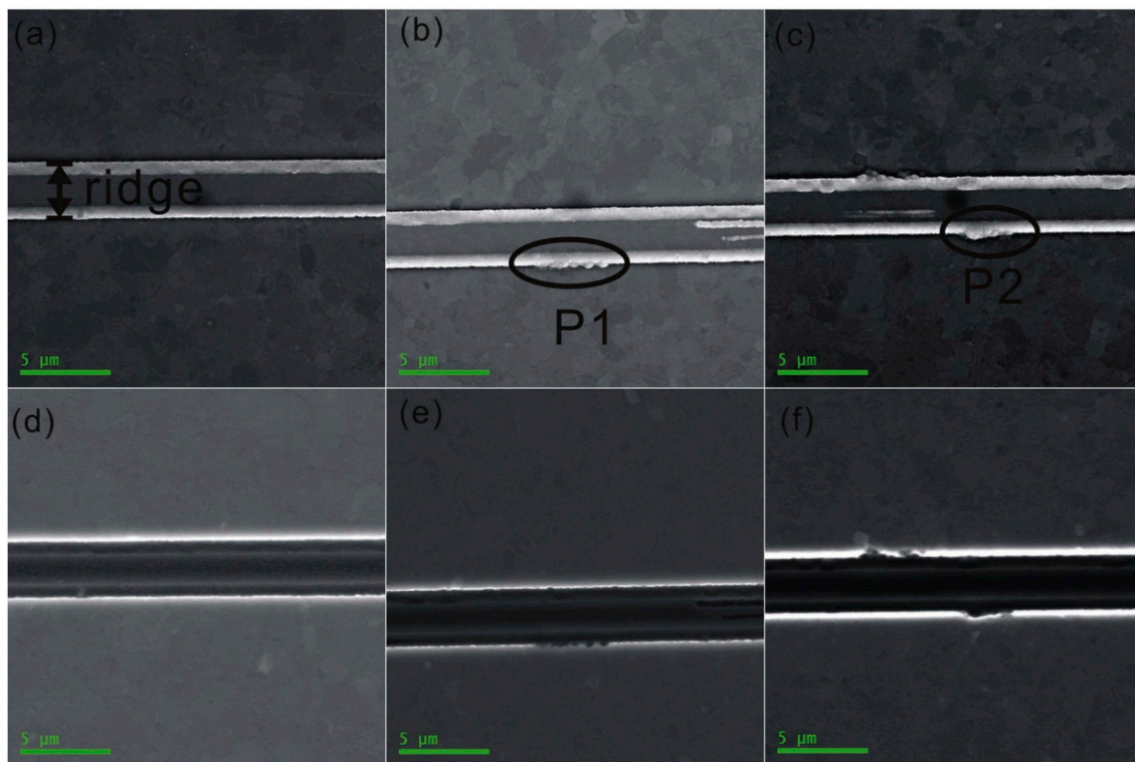


Figure 6. Typical secondary electron images of (a) non-aged LD and (b) and (c) rapidly degraded LD and the corresponding EBIC images of (d) non-aged LD and (e) and (f) rapidly degraded LD (the two black ovals mark two possible heavily degraded positions in the LD). Reprinted with permission from ref. [62] © Elsevier. Copyright 2020 Superlattices and Microstructures.

In 2007, Tatsuya Takeshita et al. of NTT, Japan, proposed a novel OBIC measurement technique to analyze the degradation position of a 2.5 Gbps directly modulated 1.55 μm uncooled DFB laser [63]. Incident beam sources with wavelengths longer than the band edge of the InGaAsP active layer were applied to improve the sensitivity of the OBIC. They confirmed that the degradation mechanism of the 1.55 μm InGaAsP/InP strained QW laser was mainly governed by diffusion defects on the waveguide rather than defects near the anti-reflective surface.

Figure 7a shows a digital OBIC scan image of the anti-reflective facet for the 1.55 μm InGaAsP/InP strained QW laser [63]. It underwent an aging time of 9000 h at 95 $^{\circ}\text{C}$. The bright areas in the figure represent the active region. To characterize the degradation of the semiconductor laser, the peak OBIC intensity of the laser was normalized to 1.0 before aging. Figure 7b shows the normalized OBIC (nor-OBIC) signal intensity profile of the laser perpendicular to the p–n junction before and after aging. The peak of the nor-OBIC intensity dropped to 0.95 after aging, which indicates the degradation of the active layer after aging.

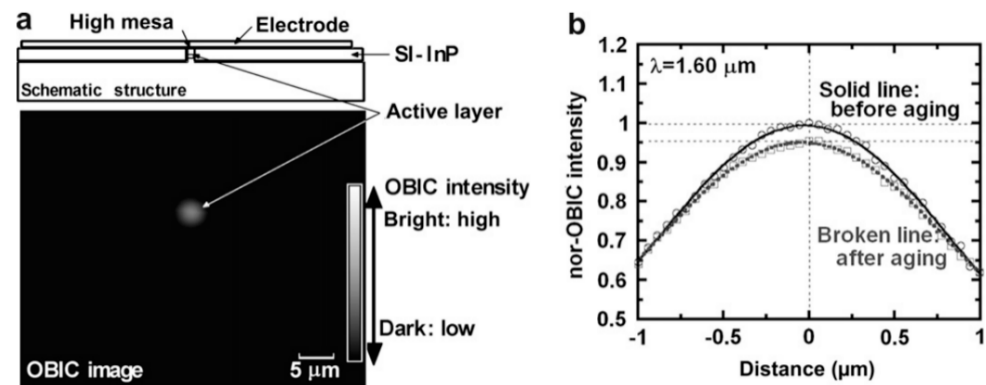


Figure 7. OBIC technique for monitoring the internal degradation of the laser. (a) OBIC image of the laser and (b) normalized OBIC signal intensity profile. Reprinted with permission from ref. [63] © Elsevier. Copyright 2007 Microelectronics Reliability.

In 2021, Che Lun Hsu et al. from National Yang Ming Chiao Tung University presented a modified OBIC microscope based on a tunable ultrafast laser to spectrally resolve the failure point of an electrostatic discharge-damaged VCSEL [64]. A spectrally resolved OBIC image of a normal VCSEL is shown in Figure 8 [64].

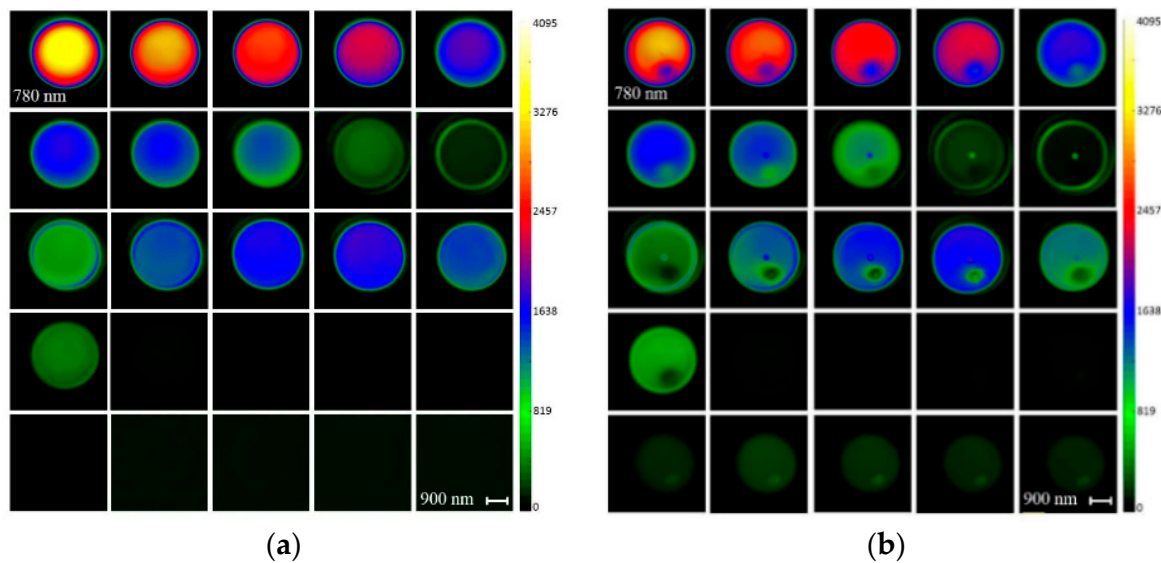


Figure 8. Spectrally resolved OBIC for ESD detection. (a) Normal and (b) Spectrally resolved OBIC image of the EDS-HBM VCSEL. Reprinted with permission from ref. [64] © The Optical Society. Copyright 2021 OSA Continuum.

The OBIC image was obtained by adjusting the incident wavelength at 5 nm intervals between 780 and 900 nm. The photocurrent signal was adjusted by a voltage preamplifier before being fed to the A/D converter for mapping. The obtained OBIC images are presented in a color-coded format. The active region of the OBIC confined by the oxide layer can be identified, resulting in a circular pattern. In a normal VCSEL (Figure 8a), the photocurrent distribution in the active region is very uniform. The maximum intensity of the photocurrent appears when the incident wavelength is 780 nm. When the incident wavelength is longer than 860 nm, there is no photocurrent response.

Figure 8b shows the spectrally resolved OBIC image of the ESD-HBM (human body model) VCSEL, in which it can be seen that there are two defect points in the active region: a large one at the edge and a small one near the center of the edge. Therefore, the OBIC technique can precisely define the damage location and failure cause of ESD-damaged VCSELs.

4.3. TIVA

Due to it being non-invasive and having a simple sample preparation, the TIVA technique is widely recognized as a fast and effective tool for locating defects in current biased devices, especially those with poor optical emission [65,66]. It is a type of thermal laser stimulation (TLS) technique. A focused 1.064 μm laser beam is used as an active probe to scan and locate defects in group III–V semiconductor lasers. The focused laser scan causes a localized change in thermal gradient at the scan location, which results in a change in local resistance. The change in resistance is captured when monitoring the voltage change across a fixed current source.

TIVA has been widely used to perform topside and backside inspections of failed VCSELs. Robert W. Herrick et al. of the Intel Corporation used the “backside TIVA” technique to inspect the DLDs in VCSELs [67]. Figure 9 shows TIVA images of mesa oxide in VCSELs before and after aging tests [67]. The reflected bright image (Figure 9a) shows a mesa with a diameter of about 42 μm and an oxide pore size of 12 μm . Figure 9b shows the TIVA image of the back side of the device under normal operation conditions. It shows some evidence of damage in the upper left corner, but it has not yet spread. The TIVA image of the degraded device (Figure 9c) shows the DLD propagating from the edge of the mesa in the lower right corner and then causing a failure as it reaches the emitting region in its center.

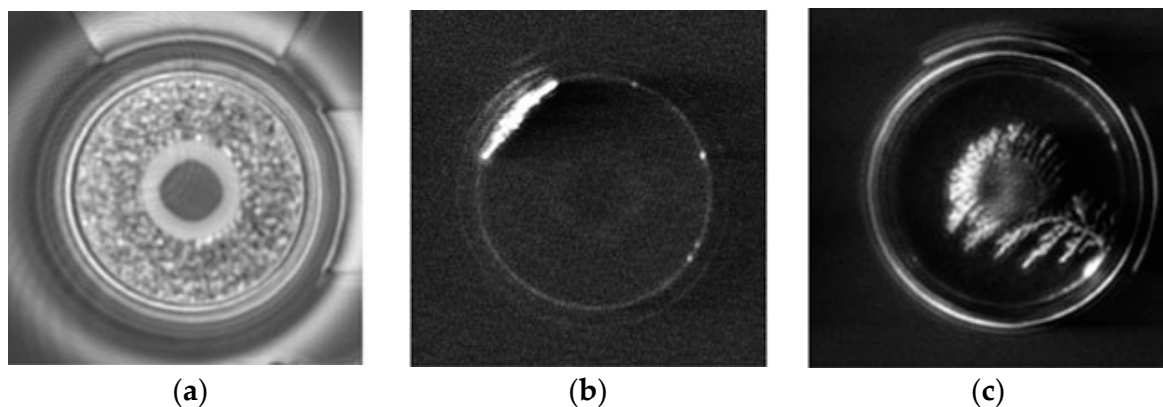


Figure 9. TIVA for detecting DLDs in VCSEL. (a) Reflected light image, (b) TIVA image of a normal VCSEL, and (c) TIVA image of a VCSEL damaged by aging test. Reprinted with permission from ref. [67] © Springer Nature. Copyright 2013 Springer eBook.

4.4. EL

EL is always employed to detect hidden cracks, black blocks, dislocations, and stacking faults in semiconductor lasers. The use of EL is usually sufficient to classify the location of the damage in EELs. When a fixed field is applied to the active region of a laser chip, the part without defects emits photons due to electron and hole recombination, while the defective part without electron and hole recombination shows a dark region. EL imaging is particularly suited to study the development of DLDs caused by luminescence-killing dislocation networks in laser cavities. EL line scans across a defect structure provide useful quantitative information.

In 2018, Yongkun Sin et al. from the Aerospace Corporation, El Segundo, found a new failure mode in high-power multi-mode InGaAs/AlGaAs strained QW lasers using EL techniques for short-term step stress tests and long-term accelerated aging tests [68]. Figure 10 shows the top surface EL images of two multi-mode InGaAs/AlGaAs strained QW lasers [68]. Figure 10a shows the DLD starting from the front mirror, indicating the degradation of the facets (COMD failure). Additionally, the DLDs of the bulk failure in Figure 10b start from the inside of the cavity, indicating catastrophic optical bulk damage (COBD failure).

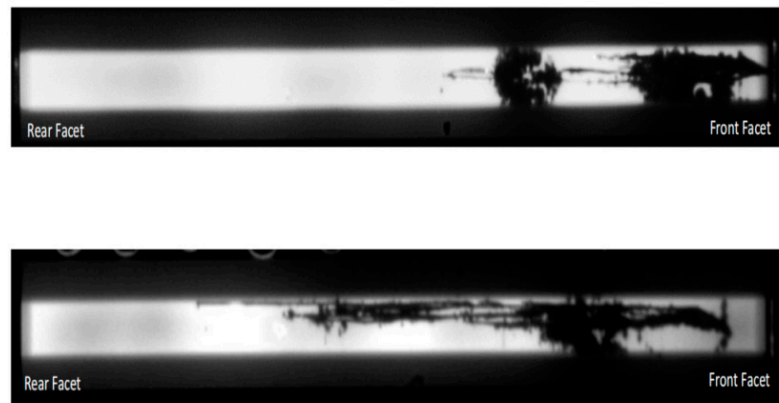


Figure 10. EL images of degraded multi-mode lasers show a facet failure and a bulk failure. Reprinted with permission from ref. [68] © Springer Nature. Copyright 2018 MRS Advances.

4.5. μ -PL Mapping

The μ -PL mapping technique is a simple, non-destructive, and non-contact method used to detect the defect concentrations and crystalline quality of semiconductor materials. The semiconductor material is irradiated by a certain frequency of light. The electrons in the defect-free parts are excited to a higher electronically excited state, and then radiate a photon as the electrons return to a lower energy state and release energy (photons). PL intensity mapping and peak wavelength mapping in semiconductor wafers as grown and processed can provide information on material uniformity, dislocation density, the density of deep traps, the distribution of residual impurities, and anneal uniformity.

In 2006, Marwan Bou Sanayeh et al. of OSRAM Opto Semiconductor GmbH employed the μ -PL mapping technique to investigate COMD-induced defects in high-power AlGaInP broad-area lasers [69]. Figure 11 shows the μ -PL mapping of the COMD laser. From the magnification of the defects near the output facet, highly non-radiative defects start from the output facet and propagate parallel to the waveguide direction inside the cavity.

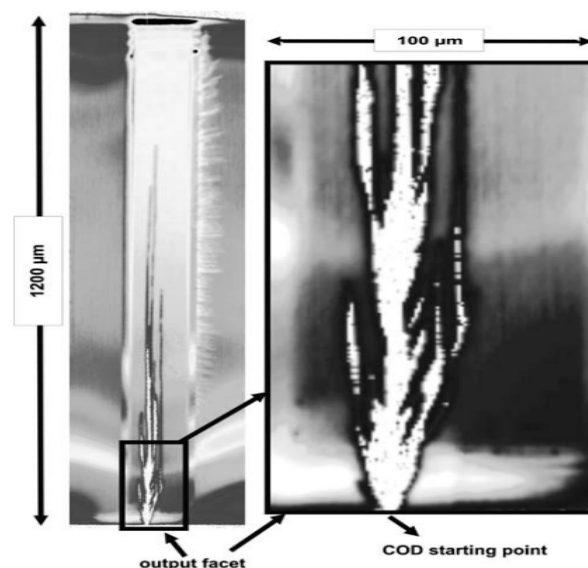


Figure 11. μ -PL mapping of a laser after COMD with a magnification of the output facet (white = low PL intensity and black = high PL intensity). Reprinted with permission from ref. [69] © AIP Publishing. Copyright 2006 Applied Physics Letters.

4.6. EMMI

The EMMI technique is a highly efficient and high-precision, non-destructive method used to detect leakage currents from device defects, ESD failures, junction leakage, contact

spiking, and hot electrons, etc. By detecting the photons excited by the recombination of electron and hole, the failure position and mechanism can be deduced. Based on the precise positioning of the EMMI, focused ion beam (FIB) slitting enables direct observation and analysis of the localization of failure points.

In 2021, Roert Fabbro et al. from AMS, Unterpremsteatten, AG, Austria, and Graz University of Technology, Graz, applied the reverse-bias EMMI technique to detect defect localization in high-power VCSEL arrays. They performed failure detection on a high-power 2D-VCSEL array consisting of 932 emitters, as shown in Figure 12a [70].

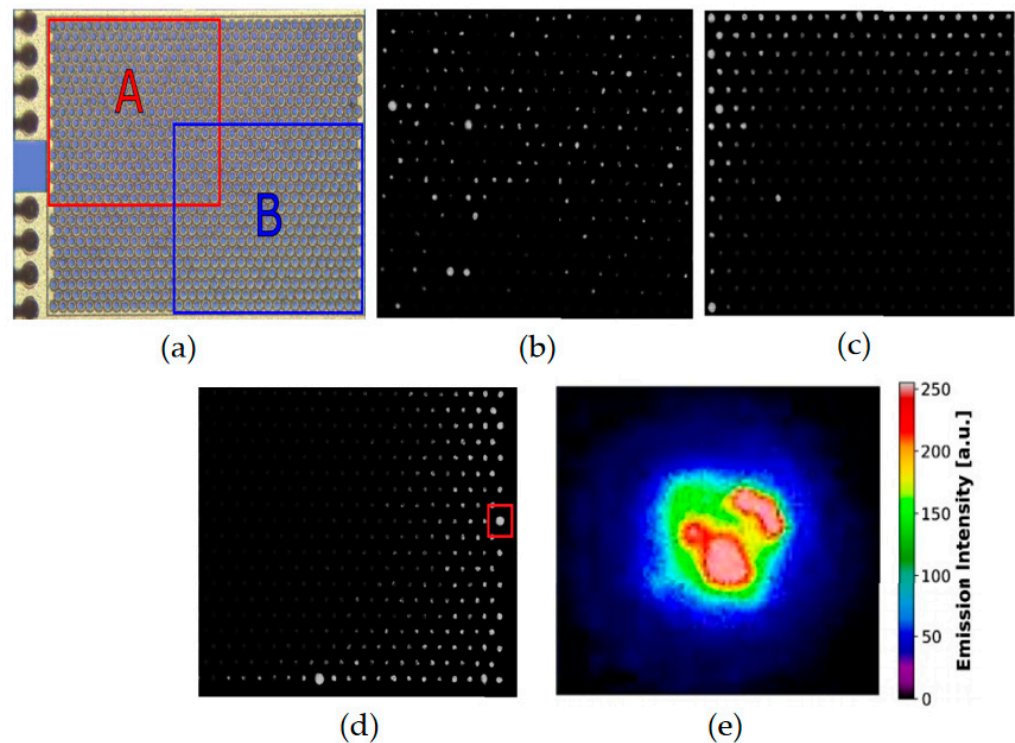


Figure 12. (a) High-power 2D-VCSEL array consisting of 932 emitters. (b) Reverse-bias EMMI image of region A of the VCSEL array before stress; (c) reverse-bias EMMI image of region A of the VCSEL array after stress; (d) reverse-bias EMMI image of region B in the VCSEL array after stress; and (e) colorized close-up of the marked emitter in (d). Reprinted with permission from ref. [70] © IOP Publishing. Copyright 2021 Measurement Science and Technology.

Figure 12b,c show the photon emission changes of individual emitters on the VCSEL array in a reverse-bias EMMI before and after stress [70]. They found that the most promising emitters showing degradation and defects were those showing a change from dark to bright (i.e., the change shown between Figure 12b,c). The emission intensity of each emitter depends on the intrinsic shunt resistance; defects such as cracks, ESD damage, and DLDs also act as leakage current pathways by damaging the internal crystal structure. These additional pathways increase the overall leakage current flowing through the emitters during PN junction reverse bias, and avalanche breakdown occurs, thus increasing the emission intensity of the damaged emitters during reverse bias. Figure 12d presents the reverse-bias EMMI image of region B in the VCSEL array after stress, where one of the emitters has high brightness (red square on the right side of the figure). A colorized close-up of the reverse-bias emission pattern of one of the emitters with a high brightness shows emissions across the whole emitter with two main defect spots (Figure 12e).

4.7. CL

The cathodoluminescence (CL) spectroscopy technique has a nanoscale spatial resolution (30–50 nm), which is normally applied to characterize the changes in composition,

strains, and crystalline defects in semiconductor materials, such as dislocations, stacking faults, and impurities, etc. It can track elements and impurities and analyze the failure causes of semiconductor materials and defect localization within lasers. The CL technique is a powerful tool for observing dislocation defects in the active region of a semiconductor laser.

Due to the interaction of high-energy electrons (cathode rays) with a semiconductor material, electromagnetic radiation or a light ranging from visible to near-infrared is created by electron transitions in bandgaps or defect localizations. Using a specialized SEM, the electromagnetic radiation or light can be collected.

In 2013, V. Hortelano from the University of Valladolid investigated the defect signatures in degraded high-power laser diodes [18]. The degradation mechanism of an aged 980 nm single-ridge waveguide InGaAs/AlGaAs-based QW laser and broad-area emitter 808 nm AlGaAs/GaAs QW laser were studied using the CL technique. The characteristics are shown in Figure 13. Figure 13a,b show the CL images of DLDs in the 980 nm InGaAs/AlGaAs QW laser. The $\langle 100 \rangle$ DLDs at 45° to the cavity and the $\langle 1-10 \rangle$ DLDs perpendicular to the cavity can be observed in Figure 13 (a) and (b), respectively. The propagation of the DLD in Figure 13a is driven by the REDC mechanism. The propagation of the DLD in Figure 13b is driven by the REDG mechanism. Figure 13c shows the V-shaped defect in an aged 808 nm AlGaAs/GaAs QW laser.

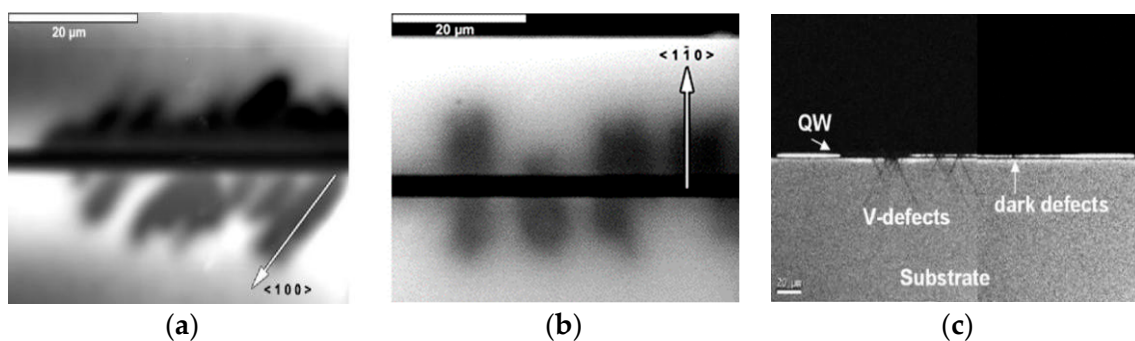


Figure 13. DLDs observed by the CL technique. (a) CL image of DLDs at 45° to the cavity, (b) CL image of DLDs perpendicular to the cavity, and (c) CL image of V-shaped defects. Reprinted with permission from ref. [18] © Elsevier. Copyright 2013 Microelectronics Reliability.

4.8. TEM

TEM is based on the interaction between a high-energy electron beam and a very thin sample. It is a high-resolution technique used to reveal the crystallographic phase at the nanometer scale; to characterize crystal defects such as dislocation, grain boundaries, voids, and stacking faults in a III–V super lattice; and to identify nanometer-sized defects on integrated circuits, including embedded particles and via residues.

In 2010, Shigetaka Tomiya et al. from Advanced Materials Laboratories, Sony Corporation, investigated the structural defects and degradation phenomena in high-power pure-blue InGaN-based laser diodes. They proposed that the 440–450 nm InGaN-based LDs were degraded by an increase in the capture cross-section of non-radiative recombination centers at the active regions due to the diffusion of point defects and/or impurities during laser operation [17].

They confirmed that the introduction of a current injection-free region at/near the laser facet had a significant effect on the suppression of COMD degradation. Additionally, the increase in non-radiative recombination centers was caused by the current injection and not by an optical effect. The multiple defects consisted of a combination of columnar defects, and dislocations were demonstrated by cross-sectional TEM images of the multiple quantum wells (MQWs).

4.9. ECCI

ECCI relies on electron diffraction inside crystalline materials. The information of the crystalline defect is carried by elastically backscattered electrons, which can be significantly modulated by the crystal orientation near the top surface. It is a helpful method used to examine the dislocation distribution and cross-sectional facet conditions of aged devices. It allows the detection and characterization of dislocation substructures near the surface of bulk specimens, which can be retested and re-examined, and it allow a large area of the specimen to be examined, thus allowing statistical information to be collected for large numbers of persistent slip bands and cracks.

The advantage of adopting the ECCI method compared to cross-sectional TEM image is that no sample preparation is required, and, moreover, one can continuously monitor the device aging process without damaging the device structure.

In 2021, Bei Shi et al. from the University of California Santa Barbara, USA, applied the ECCI technique to examine the dislocation distribution of aged 1550 nm InGaAs/InP QW laser diodes monolithically grown on silicon [20]. A high density of V-shaped defects originating from the multiple-QW region was detected before device aging. Extended DLDs were observed in the QW region, the InP buffer, and the strained-layer super lattices. They found that the DLDs introduced new misfit dislocations and promoted the climbing of threading dislocations, leading to device degradation.

4.10. Raman

Laser Raman microprobe spectroscopy is a non-destructive detection method that measures damaged portions of semiconductor materials and characterizes the compositional changes and lattice quality of the epitaxial layers [71]. It is an analytical technique in which scattered light is used to measure the vibrational energy pattern of the sample. The stresses and strains present in the sample can be obtained by comparing the changes in the peak positions of the Raman peaks; the polarization direction of Raman is used to determine the crystal symmetry and lattice orientation. By comparing the intensity of the Raman peaks, the total amount of substances in the material can also be known.

In addition to the above methods, there are many other techniques that can be applied to analyze the degradation mechanism of high-power semiconductor lasers, such as deep level transient spectroscopy (DLTS) [72,73], X-ray diffraction (XRD) [74,75], scanning electron microscope (SEM) [76], secondary ion mass spectroscopy (SIMS) [77,78], X-ray photoelectron spectroscopy (XPS) [79], and infrared thermal image detection technology (IRT) [80]. The principles of the different detection techniques are quite different, so there are big differences in the difficulty of the detection techniques, sample preparation methods, and matters needing attention.

Table 2 lists the detection category, selectivity, and technical advantages and limitations of different detection techniques. In practical applications, the advantages and strategies of the various techniques should be comprehensively considered to find the root cause of the device's failure.

Table 2. Comparison of various detection methods.

Method	Detection category	Selectivity	Advantages	Limitation
EBIC	Non-destructive (VCSEL, topside) Non-destructive (EEL, topside and front facet) Destructive (EEL, backside)	High	Detecting the DLDs, stacking faults and precipitates in the active region nearby	Defects in cladding or contact layer are not visible
OBIC	Non-destructive (VCSEL, topside) Non-destructive (EEL, topside and front facet) Destructive (EEL, backside)	High	Detecting degradation area and degree in the buried heterojunction and waveguide layers	For high-speed devices, the ability to observe the spectral response adequately is limited

Table 2. Cont.

Method	Detection category	Selectivity	Advantages	Limitation
TIVA	Non-destructive (VCSEL, topside) Non-destructive (EEL, topside)	High	Sensitive to leakage current and can detect the failure both on the surface and below	Signal might be blocked by metallic layers
EL	Non-destructive (VCSEL, topside) Non-destructive (EEL, topside and front facet) Destructive (EEL, backside)	Medium	Good at detecting the development of DLDs caused by luminescence-killing dislocation networks in the laser cavity	Not suited to detecting lasers with blanket metal over the epi-side, or mounted epi-side-down
μ -PL	Non-destructive (epitaxial wafer, topside) Non-destructive (VCSEL, topside) Non-destructive (EEL, topside) Destructive (EEL, backside)	High	Measures isolated defects and residual mechanical stress induced by the packaging process	Cannot provide information of luminescence features with dimensions below the classical diffraction limit
CL	Non-destructive (epitaxial wafer, topside) Non-destructive (VCSEL, topside) Non-destructive (EEL, topside) Destructive (EEL, backside)	High	Sensitive to the presence of non-recombination centers, high lateral and in-depth resolution	Result depends greatly on the device resistances
EMMI	Non-destructive (VCSEL, topside) Non-destructive (EEL, topside and front facet)	Medium	The luminescent defects can be located, low leakage current requirement	Poor resolution of non-luminous defects in metallic shaded areas
DLTS	Non-destructive (VCSEL, topside) Non-destructive (EEL, topside)	High	Sensitive to deep level defects, comprehensive characterization information	Cannot obtain deep energy level electron wave functions or defect internal information
Raman	Non-destructive (VCSEL, topside) Non-destructive (EEL, topside)	Medium	No need for sample processing, short time, high sensitivity	Weak signal strength
FIB-TEM	Destructive (VCSEL, topside) Destructive (EEL, topside)	High	Maximum magnification, high image quality, deep failure analysis; root cause identification	Significant sample preparation time, small sampling volumes, unable to detect the materials' instability in high-energy electron beams
XRD	Non-destructive (VCSEL, topside) Non-destructive (EEL, topside)	High	Small sample size and simple interpretation result	Susceptible to interference of mutual elements and superposition peaks
SEM	Non-destructive (epitaxial wafer, VCSEL, EEL, topside) Non-destructive (epitaxial wafer, cross-section) Non-destructive (EEL, front facet) Destructive (EEL, backside)	High	Detects failures such as delamination, oxidation contamination, and melting at the surface	Cannot detect root cause hidden below surface

Table 2. Cont.

Method	Detection category	Selectivity	Advantages	Limitation
ECCI	Non-destructive (epitaxial wafer, topside) Non-destructive (VCSEL, topside) Non-destructive (EEL, topside) Destructive (EEL, backside)	High	High precision, no need for sample preparation, allows the examination of large area of specimen	Resolution is limited by SEM system; the background signal is strong; and dislocation detection and signal analysis are prone to interference
SIMS	Destructive (epitaxial wafer, VCSEL, EEL, topside)	High	Can acquire the information of several atomic layers or even single elements	Difficulties in quantitative analysis
XPS	Non-destructive (VCSEL, topside) Non-destructive (EEL, topside)	High	Good repeatability of spectral line, fast speed and high sensitivity	Low energy resolution and low peak-to-back ratio
IRT	Non-destructive (VCSEL, topside) Non-destructive (EEL, front facet) Destructive (EEL, topside)	Medium	Strong signal and easy to measure	Large quantitative analysis errors and low sensitivity

5. Failure Improvement Measures

By analyzing the failure modes and causes of high-power semiconductor lasers, methods by which to improve the reliability of high-power semiconductor lasers are proposed in terms of the preparation process, reliability screening, and method application.

5.1. Preparation Process

To avoid internal degradation, it is very important to avoid defects caused by epitaxial growth and to minimize internal and external stresses in semiconductor lasers.

Substrates with low or no dislocation density are commercially available to avoid the propagation of threading dislocations into the active region. Designing an appropriate buffer layer or an etching stop layer can reduce the defects caused by the segregation process between atomic layers. Minimizing the oxygen content in the epitaxial growth atmosphere and selecting lattice-matched epitaxial films are useful methods by which to reduce the internal stresses and defects in laser diodes.

To reduce the external stresses in the bonding process, a low-melting-point Aurum–stannum (Au–Sn) alloy solder with strong oxidation, good thermal conductivity, and less susceptibility to metallurgical reactions can be used to replace the original Indium (In) solder. Appropriate composite heat sinks with high thermal conductivity and less thermal expansion stress can effectively improve the reliability of semiconductor lasers due to their good match with the thermal expansion efficiency of the chip. Appropriate designs of the high heat flux microchannel heat sink exchanger can be used for the cooling of semiconductor laser diode arrays. High-efficiency coupling and package technique are necessary to increase the lifetime of laser diodes.

The application of effective surface passivation; vacuum cleavage and coating techniques; or the fabrication of non-absorbing mirror structures, such as the use of QW intermixing techniques, can be used to prevent the COMD phenomenon.

5.2. Reliability Screening

High-power semiconductor lasers are generally required to operate for long periods with continuous electricity input and are subject to changes in environmental conditions (radiation, temperature, and humidity, etc.), and therefore require a high degree of reliability and stability.

To ensure the quality of the devices in the application system, semiconductor lasers must undergo rigorous inspection and aging screening prior to assembly. In the manufacturing process of lasers, early failures are usually accelerated by aging screening to screen out early failing devices and to ensure the reliability of semiconductor lasers.

Aging screening refers to the method of applying stress during the early operation of the device to accelerate the discovery of early failing devices and to screen out potential faults in time [81]. The applied stress can be thermal stress, electrical stress, mechanical stress, or a combination of different stresses. The applied stress should be controlled within an appropriate range. If it is too small, it may not achieve the screening effect, and if it is too large, it will introduce new failure causes. At present, the main methods used are high-temperature storage, high- and low-temperature shock, high-temperature power aging, mechanical vibration, centrifuge acceleration, leakage, and humidity and heat, etc., among which high-temperature power aging is the most common method [82].

The benefit of aging screening is that it can greatly reduce the risk of early failure, but it can also increase the overall production costs. For example, for a 144-pin package product, 24-h aging is used, and the cost is about 30% of the total cost [83].

Typical failure criteria of pump semiconductor lasers include, for example, a 5% reduction in ex-facet power during accelerated life tests at high temperatures and power or a 50% increase in the threshold current at the rated power [1].

5.2.1. High-Temperature Storage

High-temperature storage is a static aging mode. The devices are aged and screened after being placed in a high-temperature environment for certain time. The method mainly examines the effect of temperature on the device, which can accelerate chemical reactions on the chip's surface, the extension of defects inside the device, and the oxidation process of virtual solder joint, etc. [84]. The influences of high temperatures on the performance of the device include electrical parameter changes, heat dissipation difficulties, thermal aging, and chemical decomposition.

The devices are subjected to environmental tests of high-temperature storage between 120 °C to 300 °C; the storage time can be from dozens of hours to hundreds of hours. Generally speaking, the higher the temperature and the longer the storage time, the better the effect. The test depends on the reliability requirements of the device.

5.2.2. High- and Low-Temperature Shock

High- and low-temperature shock means that the device is stored in alternating high- and low-temperature environments without powering up the device. It is a useful way to check the match conditions of thermal expansion coefficients between different epitaxial materials. Potential quality-related problems (cracks, sealing performance, and pressure welding) can be found.

The rigor of the test depends on the selected high and low temperatures, the length of exposure time, and the number of cycles.

5.2.3. High-Temperature Power Aging

High-temperature power aging refers to a certain high-temperature stress and electrical stress on the device. It is an effective aging method used to simulate the operating conditions of the device in an actual circuit, coupled with high-temperature (+80 °C–180 °C) aging.

High-temperature power aging is suitable for filtering semiconductor lasers with surface contamination, wire welding, current leakage, cracks, oxide layer defects, and local hot spots, etc.

5.3. Method Application

When the semiconductor laser is in operation for a long time, electrical or voltage overload, electrical surges, and thermal overload often occur. These phenomena could be

decreased, such as intentionally reducing the electrical stress, thermal stress, or mechanical stress in the laser.

High-power semiconductor lasers must have good thermal resistance, and the internal and external thermal resistance of the device should be reduced as much as possible. Scratches and mechanical damage should be prevented during the operation and use of the laser diode.

It is important to minimize the generation of static electricity, for example, by designing the physical circuit of the electrostatic discharge outside the laser; by using an anti-static carpet, workbench, and clothing; or by controlling the humidity of the environment. The welding and testing instruments must be properly grounded.

6. Conclusions

This paper introduces the failure mechanisms, accelerated aging experiments, failure detection techniques, and improvement methods of high-power semiconductor lasers. It can be seen that the reliability of high-power semiconductor lasers is influenced by many factors, and the reliability can be improved by using a comprehensive analysis of multiple techniques. Choosing the right experimental aging conditions not only saves time but also reveals the correct failure mechanism in semiconductor lasers and obtains the true reliability level of the devices. Choosing the proper failure detection techniques helps one to correctly analyze the causes of failure in high-power semiconductor lasers so as to improve their lifetime and reliability.

Author Contributions: Conceptualization, Y.S., S.N. and Z.L.; methodology, J.B. and Z.W.; validation, Y.S. and Y.C.; formal analysis, L.L. and P.J.; investigation, Y.S., Z.L., S.N., and Y.L.; resources, Y.S., Z.L. and J.B.; writing—original draft preparation, Y.S., S.N. and Z.L.; writing—review and editing, Y.C.; supervision, Y.C. and L.L.; project administration, L.Q., X.S. and L.L.; funding acquisition, L.Q., X.S. and L.W. All authors have read and agreed to the published version of the manuscript.

Funding: This work was funded by National Science and Technology Major Project of China (2021YFF0700500); National Natural Science Foundation of China (NSFC) (62090051, 62090052, 62090054, 11874353, 61935009, 61934003, 61904179, 62004194); Science and Technology Development Project of Jilin Province (20200401069GX, 20200401062GX, 20200501006GX, 20200501007GX, 20200501008GX); Key R&D Program of Changchun (21ZGG13, 21ZGN23); Innovation and entrepreneurship Talent Project of Jilin Province (2021Y008); Special Scientific Research Project of Academician Innovation Platform in Hainan Province (YSPTZX202034); Lingyan Research Program of Zhejiang Province (2022C01108); Science and Technology Innovation Program of Changchun Institute of Optics, Fine Mechanics and Physics, Chinese Academy of Sciences.

Data Availability Statement: Not applicable.

Acknowledgments: The authors thank Ligong Zhang and Yongqiang Ning for helping with the article, and Chaoshuai Zhang and Bokai Zhang for their constant advice and support.

Conflicts of Interest: The authors declare no conflict of interest.

References

1. Epperlein, P.W. *Semiconductor Laser Engineering, Reliability and Diagnostics: Basic Diode Laser Engineering Principles*; John Wiley & Sons Ltd.: Hoboken, NJ, USA, 2013; pp. 35–39, 72–74, 326–332.
2. Cooper, D.P.; Gooch, C.H.; Sherwell, R.J. Internal self-damage of gallium arsenide lasers. *IEEE J. Quantum Electron.* **1966**, *2*, 329–330. [[CrossRef](#)]
3. Kressel, H.; Mierop, H. Catastrophic Degradation in GaAs Injection Lasers. *J. Appl. Phys.* **1968**, *38*, 5419–5421. [[CrossRef](#)]
4. Orton, J.W. Reliability and Degradation of Semiconductor Lasers and LEDs. *Opt. Acta Int. J. Opt.* **1992**, *39*, 1799–1800. [[CrossRef](#)]
5. Ueda, O. On Degradation Studies of III–V Compound Semiconductor Optical Devices over Three Decades: Focusing on Gradual Degradation. *Jpn. J. Appl. Phys.* **2010**, *49*, 090001–090008. [[CrossRef](#)]
6. Ueda, O. Reliability and Degradation of III–V Optical Devices. In *Materials and Reliability Handbook for Semiconductor Optical and Electron Devices*; Springer: New York, NY, USA, 2013; pp. 87–120.
7. Epperlein, P.W.; Buchmann, P.; Jakubowicz, A. Lattice disorder, facet heating and catastrophic optical mirror damage of AlGaAs quantum well lasers. *Appl. Phys. Lett.* **1993**, *62*, 455–457. [[CrossRef](#)]

8. Jakubowicz, A.; Oosenbrug, A.; Forster, T. Laser operation-induced migration of beryllium at mirrors of GaAs/AlGaAs laser diodes. *Appl. Phys. Lett.* **1993**, *63*, 1185–1187. [[CrossRef](#)]
9. Jakubowicz, A.; Oosenbrug, A. SEM/EBIC characterization of degradation at mirrors of GaAs/AlGaAs laser diodes. *Microelectron. Eng.* **1994**, *24*, 189–194. [[CrossRef](#)]
10. Ichikawa, H.; Kumagai, A.; Kono, N.; Matsukawa, S.; Fukuda, C.; Iwai, K.; Ikoma, N. Dependence of facet stress on reliability of AlGaInAs edge-emitting lasers. *J. Appl. Phys.* **2010**, *107*, 083109. [[CrossRef](#)]
11. Krueger, J.; Sabharwal, R.; Mchugo, S.; Nguyen, K.; Tan, N.; Janda, N.; Mayonte, M.; Heidecker, M.; Eastley, D.; Keever, M.; et al. Studies of ESD-related failure patterns of Agilent oxide VCSELs. *Proc. SPIE* **2003**, *4994*, 162–172.
12. Sin, Y.; Ives, N.; Lalumondiere, S.; Presser, N.; Moss, S.C. Catastrophic optical bulk damage (COBD) in high power multi-mode InGaAs-AlGaAs strained quantum well lasers. *Proc. SPIE* **2011**, *7918*, 791803-1–791803-11.
13. Pitts, O.J.; Benyon, W.; Springthorpe, A.J. Modeling and process control of MOCVD growth of InAlGaAs MQW structures on InP. *J. Cryst. Growth* **2014**, *393*, 81–84. [[CrossRef](#)]
14. Chu, S.; Nakahara, S.; Twigg, M.E.; Koszi, L.; Flynn, E.; Chin, A.; Segner, B.; Johnston, W. Defect mechanisms in degradation of 1.3- μm wavelength channeled-substrate buried heterostructure lasers. *J. Appl. Phys.* **1988**, *63*, 611–623. [[CrossRef](#)]
15. Jianping, J. *Semiconductor Laser*, 1st ed.; Publishing House of Electronics Industry: Beijing, China, 2000; pp. 330–331.
16. Jiménez, J. Laser diode reliability: Crystal defects and degradation modes. *Comptes Rendus Phys.* **2003**, *4*, 663–673. [[CrossRef](#)]
17. Tomiya, S.; Goto, O.; Ikeda, M. Structural Defects and Degradation Phenomena in High-Power Pure-Blue InGaN-Based Laser Diodes. *Proc. IEEE* **2010**, *98*, 1208–1213. [[CrossRef](#)]
18. Hortelano, V.; Anaya, J.; Souto, J.; Jimenez, J.; Perinet, J.; Laruelle, F. Defect signatures in degraded high power laser diodes. *Microelectron. Reliab.* **2013**, *53*, 1501–1505. [[CrossRef](#)]
19. Ueda, O.; Umebu, I.; Yamakoshi, S.; Kotani, T. Nature of dark defects revealed in InGaAsP/InP double heterostructure light emitting diodes aged at room temperature. *J. Appl. Phys.* **1982**, *53*, 2991–2997. [[CrossRef](#)]
20. Shi, B.; Pinna, S.; Zhao, H.; Zhu, S.; Klamkin, J. Lasing Characteristics and Reliability of 1550 nm Laser Diodes Monolithically Grown on Silicon. *Phys. Status Solidi (A)* **2021**, *218*, 2000374. [[CrossRef](#)]
21. Ahrens, R.G.; Jaques, J.J.; Piccirilli, A.B.; Camarda, R.M.; Fields, A.B.; Lawrence, K.R.; Dutta, N.K.; Luvalle, M.J. Failure mode analysis of high-power laser diodes. *Proc. SPIE* **2002**, *4648*, 30–42.
22. Epperlein, P.W. *Semiconductor Laser Engineering, Reliability and Diagnostics: A Practical Approach to High Power and Single Mode Devices*; John Wiley & Sons Ltd.: Hoboken, NJ, USA, 2013; pp. 229–231.
23. Shi, J.W. Semiconductor laser degradation and its screening. *Semicond. Optoelectron.* **1997**, *1*, 14–19.
24. Fukuda, M. Historical overview and future of optoelectronics reliability for optical fiber communication systems. *Microelectron. Reliab.* **2000**, *40*, 27–35. [[CrossRef](#)]
25. Ueda, O. Reliability issues in III–V compound semiconductor devices: Optical devices and GaAs-based HBTs. *Microelectron. Reliab.* **1999**, *39*, 1839–1855. [[CrossRef](#)]
26. Liu, Q.K.; Kong, J.X.; Zhu, L.N.; Xiong, C.; Ma, X.Y. Failure Mode Analysis of High-power Laser Diodes by Electroluminescence. *Chin. J. Lumin.* **2018**, *39*, 180–187.
27. Fukuda, M.; Mura, G. Laser Diode Reliability. *Adv. Laser Diode Reliab.* **2021**, 1–49. [[CrossRef](#)]
28. Tamm, J.W.; Ziegler, M.; Hempel, M.; Elsaesser, T. Mechanisms and fast kinetics of the catastrophic optical damage (COD) in GaAs-based diode lasers. *Laser Photonics Rev.* **2011**, *5*, 422–441. [[CrossRef](#)]
29. Yoo, J.S.; Lee, H.H.; Zory, P. Temperature rise at mirror facet of CW semiconductor lasers. *Quantum Electron. IEEE J. Quantum Electron.* **1992**, *28*, 635–639. [[CrossRef](#)]
30. Chuang, T.H.; Lin, H.J.; Wang, H.C.; Chuang, C.H.; Tsai, C.H. Mechanism of Electromigration in Ag-Alloy Bonding Wires with Different Pd and Au Content. *J. Electron. Mater.* **2014**, *44*, 623–629. [[CrossRef](#)]
31. Korhonen, M.A.; Bo/Rgesen, P.; Tu, K.N.; Li, C.Y. Stress evolution due to electromigration in confined metal lines. *J. Appl. Phys.* **1993**, *73*, 3790–3799. [[CrossRef](#)]
32. Tamm, J.W.; Tien, T.Q.; Oudart, M.; Nagle, J. Aging properties of high-power diode laser arrays: Relaxation of packaging-induced strains and corresponding defect creation scenarios. In *Proceedings of the Cleo/Europe Conference on Lasers and Electro-optics Europe, Munich, Germany, 12–17 June 2005*; IEEE: Piscataway Township, NJ, USA, 2005; p. 112.
33. Okada, H.; Nakanishi, Y.; Wakahara, A.; Yoshida, A.; Ohshima, T. 380 keV proton irradiation effects on photoluminescence of Eu-doped GaN. *Nucl. Instrum. Methods Phys. Research. B Beam Interact. Mater. At.* **2008**, *266*, 853–856. [[CrossRef](#)]
34. O’Neill, J.; Ross, I.M.; Cullis, A.G.; Wang, T.; Parbrook, P.J. Electron-beam-induced segregation in InGaN/GaN multiple-quantum wells. *Appl. Phys. Lett.* **2003**, *83*, 1965–1967. [[CrossRef](#)]
35. Yamaguchi; Masafumi; Okuda; Takeshi. Minority-carrier injection-enhanced annealing of radiation damage to InGaP solar cells. *Appl. Phys. Lett.* **1997**, *70*, 2180–2182. [[CrossRef](#)]
36. Neitzert, H.C.; Piccirillo, A.; Gobbi, B. Sensitivity of proton implanted VCSELs to electrostatic discharge pulses. *IEEE J. Sel. Top. Quantum Electron.* **2002**, *7*, 231–241. [[CrossRef](#)]
37. Mchugo, S.A.; Krishnan, A.; Krueger, J.J.; Yong, L.; Tan, N.; Osentowski, T.; Xie, S.; Mayonte, M.S.; Herrick, R.W.; Deng, Q. Characterization of failure mechanisms for oxide VCSELs. *Proc. SPIE—Int. Soc. Opt. Eng.* **2003**, *4994*, 55–66.

38. Mendizabal, L.; Verdier, F.; Deshayes, Y.; Ousten, Y.; Danto, Y.; Béchou, L. Reliability of Laser Diodes for High-rate Optical Communications—A Monte Carlo-based Method to Predict Lifetime Distributions and Failure Rates in Operating Conditions. In *Advanced Laser Diode Reliability*; Elsevier: Amsterdam, The Netherlands, 2021; pp. 79–137.
39. Mao, S.S. Acceleration model for accelerated life test. *Qual. Reliab.* **2003**, *02*, 15–17.
40. Jennifer, L.K.; Joel, G.K. Erroneous Arrhenius: Modified Arrhenius Model Best Explains the Temperature Dependence of Ectotherm Fitness. *Am. Nat.* **2010**, *176*, 227–233.
41. Kececioglu, D.; Jacks, J.A. The Arrhenius, Eyring, inverse power law and combination models in accelerated life testing. *Reliab. Eng.* **1984**, *8*, 1–9. [[CrossRef](#)]
42. Hakamipour, N. Comparison between constant-stress and step-stress accelerated life tests under a cost constraint for progressive type I censoring. *Seq. Anal.* **2021**, *40*, 17–31. [[CrossRef](#)]
43. Moser, A.; Latta, E.E. Arrhenius parameters for the rate process leading to catastrophic damage of AlGaAs-GaAs laser facets. *J. Appl. Phys.* **1992**, *71*, 4848–4853. [[CrossRef](#)]
44. Oosenbrug, A.; Latta, E.E. High-power operational stability of 980 nm pump lasers for EDFA applications. *Lasers Electro-Opt. Soc. Meet.* **1994**, *2*, 37–38.
45. Amzajerdian, F.; Meadows, B.L.; Ba Ker, N.R.; Ba Ggott, R.S.; Singh, U.N.; Kavaya, M.J. Advancement of High Power Quasi-CW Laser Diode Arrays For Space-based Laser Instruments. In *Proceedings of the SPIE's Fourth International Asia-Pacific Environmental Remote Sensing Symposium, Honolulu, HI, USA, 8–12 November 2004*; SPIE: Washington, DC, USA, 2005; Volume 5659.
46. Stephen, M.; Krainak, M.; Dallas, J. Quasi-cw Laser Diode Bar Life Tests. In *Proceedings of the SPIE—Laser-Induced Damage in Optical Materials*; SPIE: Washington, DC, USA, 1997; Volume 3244.
47. Fouksman, M.; Lehconen, S.; Haapamaa, J.; Kennedy, K.; Li, J. High-performance high-reliability 880-nm diode laser bars and fiber-array packages. *Proc. SPIE* **2006**, *6104*, 61040A-1–61040A-6.
48. Bonati, G. Exploring failure probability of high-power laser diodes. *Photonics Spectra* **2003**, *37*, 56–58.
49. Lu, G.G.; To, G.T.; Yao, S.; Shan, X.N.; Sun, Y.F.; Liu, Y.; Wang, L.J. Reliability study of high-power semiconductor lasers. *Laser J.* **2005**, *4*, 14–15.
50. Wang, D.H.; Li, Y.J.; An, Z.F. Study on step-accelerated aging of high-power semiconductor lasers. *Micro-Nanoelectron.* **2008**, *9*, 508–511.
51. Bao, L. Reliability of high performance 9xx-nm single emitter laser diodes. *Proc. SPIE-Int. Soc. Opt. Photonics* **2010**, *7583*, 758302-1–758302-10.
52. Bao, L.; Leisher, P.; Wang, J.; Devito, M.; Xu, D.; Grimshaw, M.; Dong, W.; Guan, X.; Zhang, S.; Bai, C. High reliability and high performance of 9xx-nm single emitter laser diodes. *Proc. SPIE—Int. Soc. Opt. Eng.* **2011**, *7918*, 791806.
53. Sin, Y.; Lingley, Z.; Brodie, M.; Presser, N.; Moss, S.C. Catastrophic optical bulk degradation (COBD) in high-power single- and multi-mode InGaAs-AlGaAs strained quantum well lasers. *IEEE J. Sel. Top. Quantum Electron.* **2017**, *23*, 1500813. [[CrossRef](#)]
54. Sin, Y.; Presser, N.; Lingley, Z.; Brodie, M.; Moss, S.C. Reliability, failure modes, and degradation mechanisms in high power single- and multi-mode InGaAs-AlGaAs strained quantum well lasers. *Proc. SPIE—Int. Soc. Opt. Eng.* **2016**, *9733*, 973304.
55. Wang, W.C.; Ji, H.Q.; Qi, Q.; Wang, C.L.; Ni, Y.X.; Liu, S.P.; Ma, S. Reliability study and failure analysis of high-power semiconductor lasers. *J. Lumin.* **2017**, *38*, 165–169.
56. Nie, Z.Q.; Wang, M.P.; Sun, Y.B.; Li, S.N.; Wu, D. Thermally accelerated lifetime test of conduction-cooled high-power semiconductor laser single-bar devices in CW operation mode. *J. Emit. Light* **2019**, *40*, 1136–1145.
57. Vanzi, M.; Salmini, G.; Palo, R.D. New FIB/TEM evidence for a REDR mechanism in sudden failures of 980 nm SL SQW InGaAs/AlGaAs pump laser diodes. *Microelectron. Reliab.* **2000**, *40*, 1753–1757. [[CrossRef](#)]
58. Akamatsu, B. Electron beam-induced current in direct band-gap semiconductors. *J. Appl. Phys.* **1981**, *52*, 7245–7250. [[CrossRef](#)]
59. Henoc, P.; Benetton-Martins, R.; Akamatsu, B. Ebic and CL Study of Laser Degradation. *J. De Phys. IV* **1991**, *1*, C6-317–C6-322. [[CrossRef](#)]
60. Boudjani, A.; Sieber, B.; Cleton, F.; Rudra, A. Cl and EBIC analysis of a p + –InGaAs/n-InGaAs/n-InP/n + –InP heterostructure. *Mater. Sci. Eng. B* **1996**, *42*, 192–198. [[CrossRef](#)]
61. Sin, Y.; Ayvazian, T.; Brodie, M.; Lingley, Z. Catastrophic optical bulk degradation in high-power single- and multi-mode InGaAs-AlGaAs strained QW lasers: Part II. *Proc. SPIE* **2018**, *10514*, 10514-1–10514-14.
62. Xiu, H.; Xu, P.; Wen, P.; Zhang, Y.; Yang, J. Rapid degradation of InGaN/GaN green laser diodes. *Superlattices Microstruct.* **2020**, *142*, 106517. [[CrossRef](#)]
63. Takeshita, T.; Iga, R.; Yamamoto, M.; Sugo, M. Analysis of interior degradation of a laser waveguide using an OBIC monitor. *Microelectron. Reliab.* **2007**, *47*, 2135–2140. [[CrossRef](#)]
64. Hsu, C.L.; Das, S.; Wu, Y.S.; Kao, F.J. Spectrally resolved optical beam induced current imaging of ESD induced defects on VCSELs. *OSA Contin.* **2021**, *4*, 711–719. [[CrossRef](#)]
65. Cole, E.I., Jr.; Tangyonyong, P.; Benson, D.A.; Barton, D.L. TIVA and SEI developments for enhanced front and backside interconnection failure analysis. *Microelectron. Reliab.* **1999**, *39*, 991–996. [[CrossRef](#)]
66. Reissner, M. Fault localization at high voltage devices using thermally induced voltage alteration (TIVA). *Microelectron. Reliab.* **2007**, *47*, 1561–1564. [[CrossRef](#)]
67. Herrick, R.W. Reliability and degradation of vertical-cavity surface-emitting lasers. In *Materials and Reliability Handbook for Semiconductor Optical and Electron Devices*; Ueda, O., Pearton, S.J., Eds.; Springer: New York, NY, USA, 2013; pp. 195–197.

68. Yongkun, S.; Zachary, L.; Talin, A.; Miles, B.; Neil, I. Catastrophic Optical Bulk Damage—A New Failure Mode in High-Power InGaAs-AlGaAs Strained Quantum Well Lasers. *Mrs Adv.* **2018**, *3*, 3329–3345.
69. Sanayeh, M.B.; Jaeger, A.; Schmid, W.; Tautz, S.; Brick, P.; Streubel, K.; Bacher, G. Investigation of dark line defects induced by catastrophic optical damage in broad-area AlGaInP laser diodes. *Appl. Phys. Lett.* **2006**, *89*, 10111. [[CrossRef](#)]
70. Fabbro, R.; Haber, T.; Fasching, G.; Coppeta, R.; Michael, P.; Werner, G. Defect localization in high-power vertical cavity surface emitting laser arrays by means of reverse biased emission microscopy. *Meas. Sci. Technol.* **2021**, *32*, 095406. [[CrossRef](#)]
71. Peng, J.; Li, Q.; Xing, Z.; Zhang, J.; Ning, Y.Q. Reliability Study of Grating Coupled Semiconductor Laser Based on Raman Spectra Technique. *Spectrosc. Spectr. Anal.* **2016**, *36*, 1745–1748.
72. Yamasaki, K.; Yoshida, M.; Sugano, T. Deep Level Transient Spectroscopy of Bulk Traps and Interface States in Si MOS Diodes. *Jpn. J. Appl. Phys.* **1979**, *18*, 113–122. [[CrossRef](#)]
73. Shin, Y.C.; Dong, H.; Kang, J.; Chang, Y.K.; Kim, T.G. Optimization of 660-nm-Band AlGaInP Laser Diodes by Using Deep-Level Transient Spectroscopy Analyses. *J. Korean Phys. Soc.* **2007**, *50*, 866–870. [[CrossRef](#)]
74. Evtikhiev, V.P.; Kotel’Nikov, E.; Kudryashov, I.V.; Tokranov, V.E.; Faleev, N.N. Correlation between the reliability of laser diodes and the crystal perfection of epitaxial layers estimated by high-resolution x-ray diffractometry. *Semiconductors* **1999**, *33*, 590–593. [[CrossRef](#)]
75. Qiao, Y.B.; Feng, S.W.; Xiong, C.; Wang, X. Spatial hole burning degradation of AlGaAs/GaAs laser diodes. *Appl. Phys. Lett.* **2011**, *99*, 103506. [[CrossRef](#)]
76. Fernández-Caballero, A. A Review on Machine and Deep Learning for Semiconductor Defect Classification in Scanning Electron Microscope Images. *Appl. Sci.* **2021**, *11*, 9508.
77. Shin, Y.C.; Kim, B.J.; Dong, H.K.; Kim, Y.M.; Kim, T.G. Investigation of Zn diffusion by SIMS and its effects on the performance of AlGaInP-based red lasers. *Semicond. Sci. Technol.* **2005**, *21*, 35. [[CrossRef](#)]
78. Zhou, Q.; Li, J.Y.; Liang, H.D.; Wu, C.P. Recent developments on secondary ion mass spectroscopy. *J. Chin. Mass Spectrom. Soc.* **2004**, *25*, 113–120.
79. Yamamoto, S.; Matsuda, I. Time-Resolved Soft X-ray Photoelectron Spectroscopy: Real-Time Observation of Photo-Excited Carriers at Semiconductor Surfaces. *Hyomen Kagaku* **2016**, *37*, 9–13. [[CrossRef](#)]
80. Xie, J.; Xu, C.; Huang, W.; Chen, G. An infrared thermal image processing framework based on superpixel algorithm to detect cracks on metal surface. *Infrared Phys. Technol.* **2014**, *67*, 266–272.
81. Kuo, W.; Yue, K. Facing the headaches of early failures: A state-of-the-art review of burn-in decisions. *Proc. IEEE* **1983**, *71*, 1257–1266. [[CrossRef](#)]
82. Guijun, H.; Jiawei, S.; Yinbing, G.; Xiaosong, Y.; Jing, L. Noise as reliability screening for semiconductor lasers. *Appl. Phys. B* **2003**, *76*, 359–363. [[CrossRef](#)]
83. Zhang, L.P. The Screening Method for Early Failure of Semiconductor Devices. *Manag. Technol. SME* **2021**, *9*, 137, 138, 141.
84. Lee, J.M.; Min, B.G.; Ju, C.W.; Ahn, H.K.; Lim, J.W. High temperature storage test and its effect on the thermal stability and electrical characteristics of AlGaN/GaN high electron mobility transistors. *Curr. Appl. Phys.* **2016**, *17*, 157–161. [[CrossRef](#)]